



5-4-11

OBSERVATION AND ANALYSIS OF EARTHQUAKE MOTIONS IN AND AROUND THE SRC BUILDING AS LOCAL EARTHQUAKE INSTRUMENT ARRAY SYSTEM

Toshihide KASHIMA¹ and Yoshikazu KITAGAWA¹

¹International Institute of Seismology and Earthquake Engineering,
Building Research Institute, Ministry of Construction,
1 Tatehara, Tsukuba-shi, Ibaraki 305, Japan

SUMMARY

In this paper, the relations between the distances of observation points and the differences of earthquake motion characteristics at several points on ground surface were investigated. As the distance of observation points becomes greater, the correlation of earthquake motion characteristics becomes worse in the high frequency range. The limit frequency, in which ground motion characteristics can be regarded as identical, is related to the shear wave velocity of ground surface soil. Also, the stiffness and the damping factor of soil-structure interaction system were estimated from the observed data and the adequacy and the fluctuation of these values was investigated.

INTRODUCTION

Earthquake motions, which are observed on the ground, are affected not only by the earthquake process itself but by the propagating path of seismic waves and local characteristics of ground surface layers as well. These factors apparently influence the type of structural damages. One of the most important problems in earthquake engineering is to investigate the dynamic behavior of an actual building subjected to earthquake motions through the soil-structure interaction system.

OUTLINE OF OBSERVATION SYSTEM

Soil Profile The Building Research Institute (BRI), Ministry of Construction, is located in the northern part of the Kanto Area, the middle of Japan. Observation is carried out in the main office building and its surrounding subsoil¹⁾. The profile of the soil layers and the distribution of the shear wave velocities are shown in Fig.1. The shear wave velocities which are indicated by solid lines were given by elastic wave measurement and the others were evaluated from N-values using the equation of Goto and Ohta²⁾. A hard gravel layer appears at 96 meters below the ground surface level and a seismometer is placed on this layer, which is the deepest one. Fourier spectral ratios between accelerograms on the ground surface and at 96 meters below are shown in Fig.2 with a theoretical transfer function of the SH wave. The first predominant frequency is 0.9 Hz.

Outline of the Building The BRI main building is a seven-storey steel reinforced concrete structure with a one-storey basement and a penthouse. It is 57.6 meters in the longitudinal and 18 meters in the transverse direction. It is located longitudinally in the EW direction. The building is supported with the

mat foundation 8.8 meters deep below the ground surface. At the east end, the building is connected to a two-storey reinforced concrete building with the expansion joint. Judging from the spectral ratio of microtremors and earthquake observation records, the first natural frequencies are 2.7 Hz in the longitudinal direction and 1.8 Hz in the transverse direction.

Observation Instruments At present, array observations are done with seismometers of 17 components in the building and 37 components in the subsoil, as shown in Fig.3. Seismometers are the TUSS type and their natural frequency is 5.0 Hz. Seismographs are digitized and recorded on a magnetic tape. The absolute time is corrected automatically to the Japanese standard time by receiving the time signal broadcasted by NHK (Japanese Broadcast Corporation).

DIFFERENCES OF EARTHQUAKE MOTIONS OBSERVED ON DISTANT POINTS

In order to determine the limit frequency which is regarded as identical ground motion, differences of ground motion characteristics were investigated using seismographs which were observed at four points on the ground surface. These are A, B, D and E points in Fig.3. Three earthquakes which occurred in 1985 and 1986 were selected for this study. Specifications of the earthquakes and accelerograms on the ground surface are shown in Table 1 and Fig.4. Maximum accelerations are roughly equal but envelope curves of accelerograms vary greatly. Figure 5 shows the coherence functions of the accelerograms between distances of 25, 75 and 175 meters. As the distance between two points gets greater, the frequency at which coherence functions fall becomes lower.

The frequency where the coherence function value falls lower than 0.9 is defined as the limit frequency. Figure 6 shows the relation between the distances of observation points and the limit frequencies. In Fig.6, the solid line shows the relation of shear wave length (D) to the frequency (f) in the surface layer (shear wave velocity; $V_s=100\text{m/sec}$) - i.e., $f=V_s/D$. The limit frequencies correspond well to this equation. Therefore, the limit frequencies that can be treated as the same input earthquake motion into a building can be supposed from the width of the building and shear wave velocity of the supporting soil layer. In the case of this building, these are around 10 Hz in the longitudinal, and 3.5 Hz in the transverse direction.

ESTIMATION OF SPRING CONSTANTS AND DAMPING FACTORS

Analytical Model The soil-structure interaction system is represented by a swaying-rocking model as shown in Fig.7. In this model, a displacement at the top of the building is expressed by adding up the relative displacement components of the swaying, the rocking and the building. Assuming that the basement floor is stiff, each displacement component can be calculated from observation records of five points shown in Fig.7. This method is employed on the transverse direction in which the rocking has a notable influence.

Spring Constants Judging from the spectral ratio between observation records at the top of the building and on the ground surface, the first natural frequency of the interaction system with swaying and rocking is about 1.7 Hz. The swaying and the rocking spring constants were calculated from inertia force and each displacement component which was estimated by the above method. Here the displacement was evaluated using the FFT Method with a band-pass filter.

Figures 8 and 9 show the swaying and the rocking constants at each peak point of displacement at the top of the building. Compared with the rocking, the swaying has a greater fluctuation of spring constants depending on the kind of earthquakes and the time. The average value and the standard deviation of each

spring constant are shown in Table 2. This Table also shows the values calculated in accordance with the solutions of Yamahara³⁾ for a half space elastic soil. The spring constants obtained from observation records are 0.3-1.5 times of the theoretical value in case of swaying, and 0.8-1.1 times in case of rocking. Such differences may be caused by the amplitude levels and the durations of the earthquake motions, consequences of the layered soil, effects of the embedment, and so on.

Damping Factor Each damping factor was estimated from the damping factor of the whole interaction system by weighting with strain energy. The strain energy of each part was calculated from the spring constant and the displacement. Here damping factors of the swaying-rocking-building system and of the rocking-building system were evaluated from the spectral ratios by the Power Method, and the damping factor of the building was assumed to be 1% based on experimental results of the past.

Figure 10 shows the time sequence of the damping factors of the swaying and the rocking. The fluctuation of each damping factor due to the kind of earthquakes and to the time is great in the swaying, small in the rocking. Table 2 shows the averages and the standard deviations of the damping factors. The damping factors obtained from the observation data are 0.3-1.5 times those of the theoretical value in the swaying, 1.1-2.1 times those in the rocking. The reasons may be that the damping factors of the systems were assumed to be constants not affected by time, and that the embedding effects were not considered.

Response Analysis Using the spring constants and damping factors obtained from the observation records and the theory, the seismic response analyses were carried out. Figure 11 shows the acceleration waveform observed at the top of the building and the results of the response analyses in the case of EQ8602 (see Table 1). The response waveform with the constants obtained from the observation data corresponds well to the observed waveform.

CONCLUSIONS

Several constants were estimated from the observation records and the adequacy of these values was investigated. The results are summarized as follow:

1. The limit frequencies where frequency characteristics of input motions can be regarded as the same are estimatable from the width of the building and the shear wave velocity of the surface soil. In the case of the BRI main building, 10 Hz in the longitudinal, and 3.5 Hz in the transverse direction.
2. Spring constants and damping factors of the soil-structure interaction system can be dynamically estimated from observation records. The fluctuation of swaying constants is greater than the rocking constants.

ACKNOWLEDGMENTS

We thank Mr. H. Murata for several useful advices. We are grateful the persons concerned for their help.

REFERENCES

- 1) Kitagawa, Y., Murata, H., et al. "Observation and Analysis of Earthquake Motions in and around the SRC Building", Summaries of Technical Papers of Annual Meeting, Architectural Institute of Japan, 571-574, (1981) (in Japanese)
- 2) Goto, N. and Ohta, Y. "Construction of Empirical Formulas for Estimating Shear

Wave Velocity in Terms of Soil Indexes", Natural Disaster Material Analysis, 66-73, (1977) (in Japanese)

- 3) Yamahara, H. "Practical Solutions for Soil-Structure Interaction System", Shimizu Technical Report No.1, (1971)

Table 1 List of Earthquakes

Name	Date Time	Location of Epicenter	Magnitude Depth(km)	Δ^* (km) θ^{**} (deg)	Max.Acc. (gal)
EQ8544	'85/11/22 13:17	SE of Ibaraki pref.	4.9 56	14 -131	EW; 16.3 NS; 24.5
EQ8602	'86/02/12 11:59	off Ibaraki pref.	6.1 43	92 71	EW; 20.8 NS; 14.5
EQ8620	'86/06/24 11:53	SE off Boso pen.	6.5 73	156 158	EW; 14.3 NS; 14.5

* ; Epicentral Distance
** ; Epicentral Direction (clockwise from the N-direction)
Max.Acc ; Observed on the Ground Surface

Table 2 Average of Spring Constant and Damping Factor

	Swaying		Rocking	
	Spring Const. k_S (10^3 t/cm)	Damping factor h_S (%)	Spring Const. k_R (10^9 t*cm)	Damping Factor h_R (%)
EQ8544	7.3 (1.8)	6.6 (0.3)	35.4 (5.9)	18.9 (4.5)
EQ8602	12.1 (5.5)	19.1 (10.5)	30.6 (3.1)	20.9 (4.5)
EQ8620	14.4 (6.3)	30.4 (21.5)	36.0 (3.5)	35.5 (6.2)
Theory	12.3	21.0	35.7	17.0

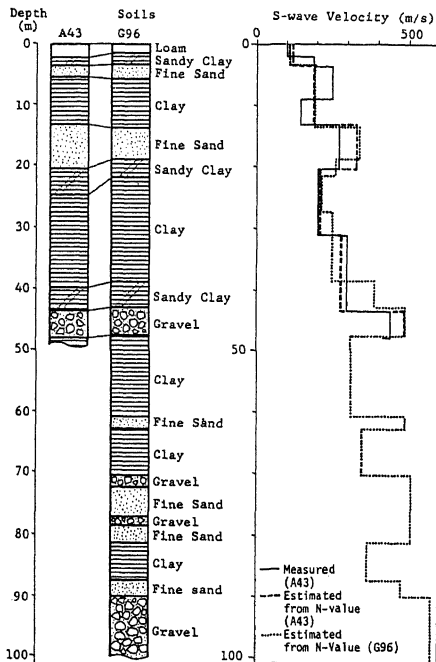


Fig. 1 Soil Profile and Shear Wave Velocities

values in () ; standard deviations

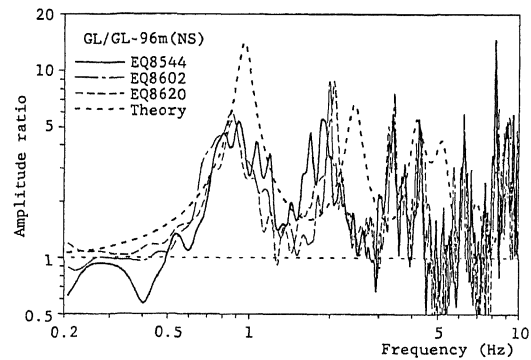


Fig. 2 Transfer functions (GL/GL-96m)

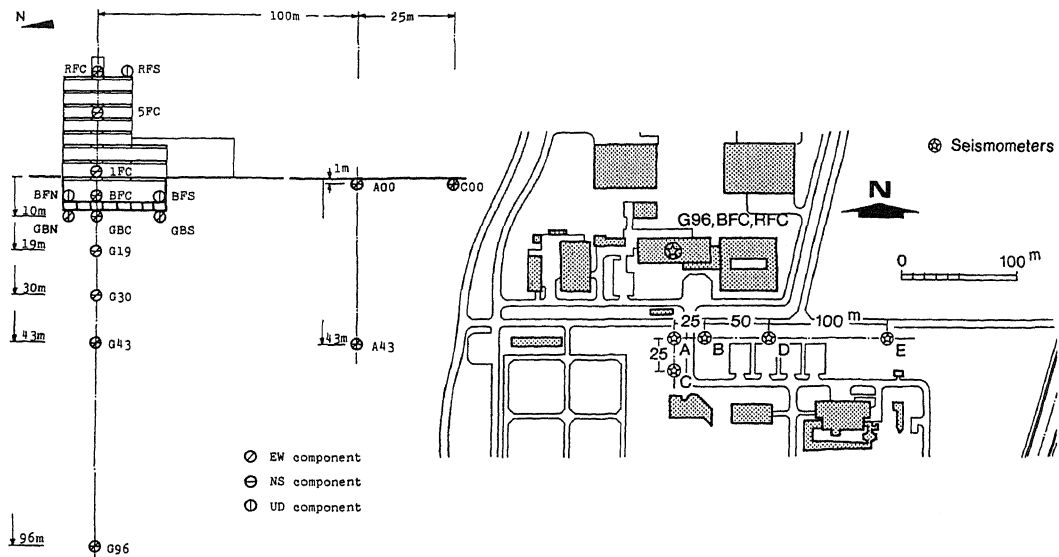


Fig. 3 Location of Seismometers

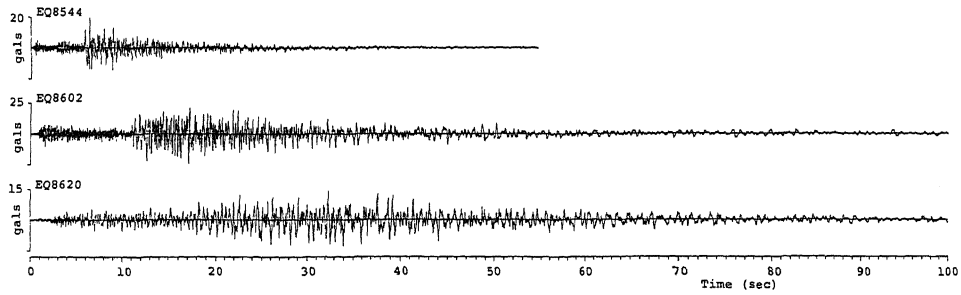


Fig. 4 Accelerograms on Ground Surface

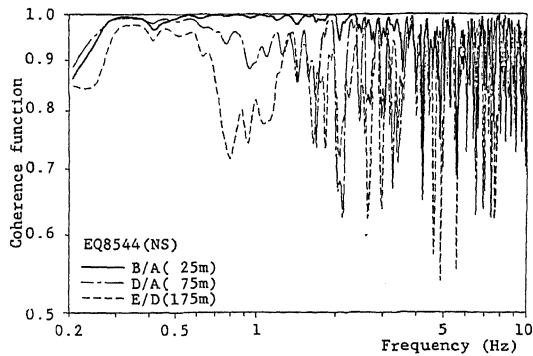


Fig. 5 Coherence Functions of Different Distances

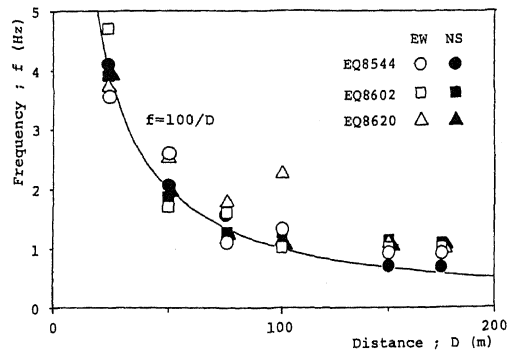


Fig. 6 Relation between Distances and Limit Frequencies

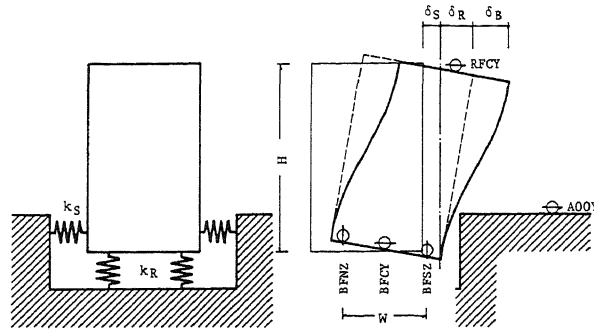


Fig. 7
Swaying-Rocking Model

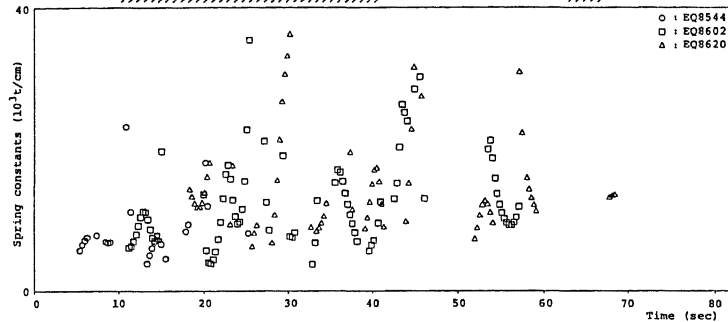


Fig. 8
Swaying Spring Constants

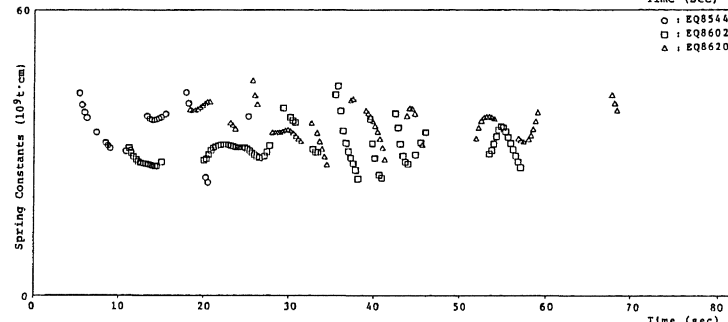


Fig. 9
Rocking Spring Constants

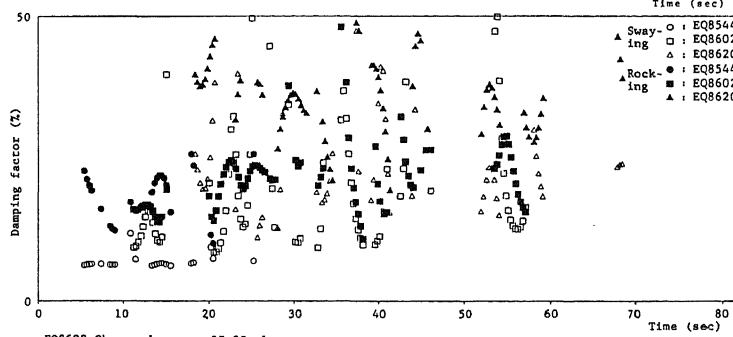


Fig. 10
Swaying and Rocking Damping factors

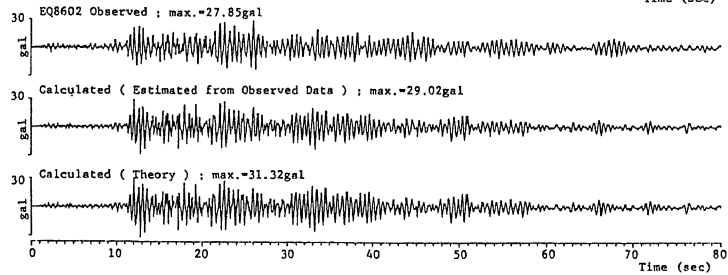


Fig. 11
Response Accelerograms at the Top of Building